environmental microbiology

Environmental Microbiology (2021) **23**(9), 5605–5620 doi:10.1111/1462-2920.15717

# *Vibrio splendidus* persister cells induced by host coelomic fluids show a similar phenotype to antibiotic-induced counterparts

**Yanan Li,[1,2] Thomas K. Wood [3], Weiwei Zhang [1,2] and Chenghua Li [1,2,4]***

[1]*State Key Laboratory for Quality and Safety of Agro-products, Ningbo University, Ningbo, 315211, China.*

[2]*Collaborative Innovation Center for Zhejiang Marine High-efficiency and Healthy Aquaculture, Ningbo University, Ningbo, 315211, China.*

[3]*Department of Chemical Engineering, Pennsylvania State University, University Park, PA, 16802.*

[4]*Laboratory for Marine Fisheries Science and Food Production Processes, Qingdao National Laboratory for Marine Science and Technology, Qingdao, 266071, China.*

## Summary

**Persister cells are dormant variants of regular cells that are multidrug tolerant and have heterogeneous phenotypes; these cells are a potential threat to hosts because they can escape the immune system or antibiotic treatments and reconstitute infectious. Skin ulcer syndrome (SUS) frequently occurs in the sea cucumber (*Apostichopus japonicus*), and *Vibrio splendidus* is one of the main bacterial pathogens of SUS. This study found that the active cells of *V. splendidus* became persister cells more readily in the presence of *A. japonicus* coelomic fluids. We showed that the *A. japonicus* coelomic fluids plus antibiotics induce 100-fold more persister cells in *V. splendidus* compared with antibiotics alone via nine sets of experiments including assays for antibiotic resistance, metabolic activity, and single-cell phenotypes. Furthermore, the coelomic fluids-induced persister cells showed similar phenotypes as the antibiotic-induced persister cells. Further investigation showed that guanosine pentaphosphate/tetraphosphate (henceforth ppGpp) and SOS response pathway involved in the formation of persister cells as determined using real-time RT-PCR. In addition, single-cell observations showed that, similar to the antibiotic-induced *V. splendidus* persister cells, the coelomic fluids-induced persister cells have five resuscitation phenotypes: no growth, expansion, elongation, elongation and then division, and elongation followed by death/disappearance. In addition, dark foci formed in the majority of persister cells for both the antibiotic-induced and coelomic fluids-induced persister cells. Our results highlight that the pathogen *V. splendidus* might escape from the host immune system by entering the persister state during the process of infection due to exposure to coelomic fluids.**

Received 15 June, 2021; revised 28 July, 2021; accepted 10 August, 2021. *For correspondence. E-mail lichenghua@nbu.edu.cn. Tel: 86-574-87609880, Fax: 86-574-87600551



## Introduction

Persister cells are a small subpopulation of dormant or slowly growing phenotypic variants in a bacterial population (Balaban, 2011; Zhang, 2014). Unlike antibiotic resistance, which generally results from genetic mutations or plasmid transfer, persister cells do not undergo genetic change (Toprak *et al*., 2011). Persister cells cause a major worldwide public health problem, because their antibiotic tolerance, combined with their ability to reinitiate growth after treatment, may result in therapy failure and relapse of infection (Michiels *et al*., 2016). Persister cells are thought to be ubiquitous among almost all bacterial species, such as *Escherichia coli* (Goormaghtigh *et al*., 2018), *Mycobacterium tuberculosis* (Dhillon *et al*., 2014), *Pseudomonas aeruginosa* (Long *et al*., 2019), *Staphylococcus aureus* (Bui *et al*., 2017), and *Salmonella enterica* serovar Typhimurium (*Salmonella Typhimurium*) (Stapels *et al*., 2018). Persister cells are reported to have distinct physiologies and phenotypic characteristics, leading to different dormancy depths that contribute to their resuscitation heterogeneity within bacterial populations (Kim *et al*., 2018; Pu et al., 2019; Wilmaerts *et al*., 2019). Bacterial persister cells may arise stochastically in unstressed bacterial cultures, but the majority of persister cell formation is promoted by environmental stress, social interaction (quorum sensing),

biofilm microenvironments, and host–pathogen interaction (Maisonneuve and Gerdes, 2014). Mechanistically, the formation and resuscitation of persister cells depend on protein level and ribosome activity (Kwan *et al*., 2013; Wood *et al*., 2019; Song and Wood, 2020).

*Vibrio splendidus* is a gram-negative bacterium that is ubiquitous in marine coastal and brackish environments (Zhang and Li, 2021). It is an opportunistic pathogen that causes severe vibriosis in a variety of marine animals (Torresi *et al*., 2011). The bacterium *V. splendidus* has been associated with the mortality of oyster (*Crassostrea gigas*) (Cao *et al*., 2018), scallop (*Argopecten purpuratus*) (González *et al*., 2017), turbot (*Scophthalmus maximus*) (Thomson *et al*., 2005), and other marine animals worldwide. Importantly, *V. splendidus* is the main pathogen that causes skin ulcer syndrome (SUS) in sea cucumber (*Apostichopus japonicus*) (Liu *et al*., 2010), which results in considerable economic losses to the aquaculture industry. Temperature, nutrient limitation, light stress, biofilm, and host stress are pressures endured by *Vibrio* spp. (Huq *et al*., 2008; Vezzulli *et al*., 2009). Faced with these challenges, *Vibrio* spp. exhibit a series of adaptive responses that allow them to persist under unfavourable environments (Vezzulli *et al*., 2009). For example, persister, a subpopulations of *Vibrio cholerae*, forms upon shedding to the aquatic environment (Silva-Valenzuela *et al*., 2017), and *Vibrio vulnificus* and *E. coli* survive in human serum in the form of persister cells (Ayrapetyan *et al*., 2015a,b). Also, *P. aeruginosa* survives in serum and can induce the expression of its antibiotic efflux pump and OprD porin, enhancing its antibiotic resistance during infection (Skurnik *et al*., 2013). Toxin/antitoxin system (TA) of *Salmonella* is activated allowing persister cell to survive vacuolar acidification and nutrient deprivation of macrophages (Helaine *et al*., 2014). When shielded from biofilms or inside host cells, persister cells are also difficult to eradicate despite prolonged antibiotic treatment (Lewis, 2005; Helaine *et al*., 2014; Wilmaerts *et al*., 2019).

The coelomic fluids of *A. japonicus* can resist the invasion of pathogenic bacteria. Our previous study showed that majority of cells of *V. splendidus* AJ01 can be eliminated by coelomic fluids (Zhang *et al*., 2016a), but whether the survivors are persister cells remains unknown. In support of this, we observed a small subpopulation within *V. splendidus* bacterial population that could survive when challenged with lethal antibiotic treatments. Moreover, co-incubation of *A. japonicus* coelomic fluids and *V. splendidus* cells increases the antibiotic tolerance of *V. splendidus*. In this study, we demonstrate that *V. splendidus* persister cells indeed form after contact with coelomic fluids via nine sets of experiments including antibiotic resistance, metabolic activity, and single-cell phenotypes.

## Results

### *Coelomic fluids induced the formation of persister cells*

In time dependent antibiotic experiments, the biphasic mode of killing indicated that persister cells were formed in the bacterial population with 10× minimum inhibitory concentration (MIC) ciprofloxacin, a gyrase inhibitor (Sanders, 1988), and 10xMIC tetracycline, a translation inhibitor (Lewis, 2005; Kwan *et al*., 2013; Cui *et al*., 2018) (Supporting Information Fig. S1). After 12 h treatment with 20× MIC of ciprofloxacin or tetracycline, $2.5 \times 10^3$ CFU·ml$^{-1}$ and $1.7 \times 10^2$ CFU·ml$^{-1}$ cells survived, respectively (Fig. 1A and B).

For comparison, we investigated the ability of coelomic fluids to induce the formation of persister cells as a pretreatment. First, the toxicity of coelomic fluids was assayed; *V. splendidus* AJ01 exponential-phase cells were incubated in fresh 2216E medium, PBS, heat-inactivated coelomic fluids (HCF), or coelomic fluids, and incubated statically at 28°C. Most of the cells survived coelomic fluids during the first hour (Fig. 1C); however, after prolonged incubation (>1 h), viable cell numbers decreased in the presence of coelomic fluids (Fig. 1C), whereas cell growth was observed in the negative control as indicated by the increased CFU counts in 2216E medium and heat-inactivated coelomic fluids (Fig. 1C). Hence, coelomic fluids were toxic to *V. splendidus*. Furthermore, stationary-phase cells (harvested at $OD_{600}$ of 1.0–1.6) could survive coelomic fluids better (Fig. 1D).

Critically, the percent of persister cells after the coelomic fluids pretreatment was increased to 14% and 19%; i.e., the portion of persister cells was 60-fold to 100-fold higher compared with antibiotic-alone induced persister cells (0.23% and 0.17%), respectively (Fig. 1E). These results show that pre-treatment of *V. splendidus* with coelomic fluids induces substantially more persister cells.

### *Coelomic fluids-induced dormant, bona fide persister cells*

Initially, dormancy was tested directly by observing single persister cells on agar gel pads that lack nutrients (Kim *et al*., 2018). Unlike exponential-phase cells, which divided (12%) or elongated (4%), none of the antibiotic-induced or coelomic fluids-induced persister cells divided or elongated on 2216E agar nutrient-free gel pads in 24 h (Supporting Information Fig. S2 and Table S2). These results reveal that the antibiotic-induced and coelomic fluids-induced persister cells are dormant.

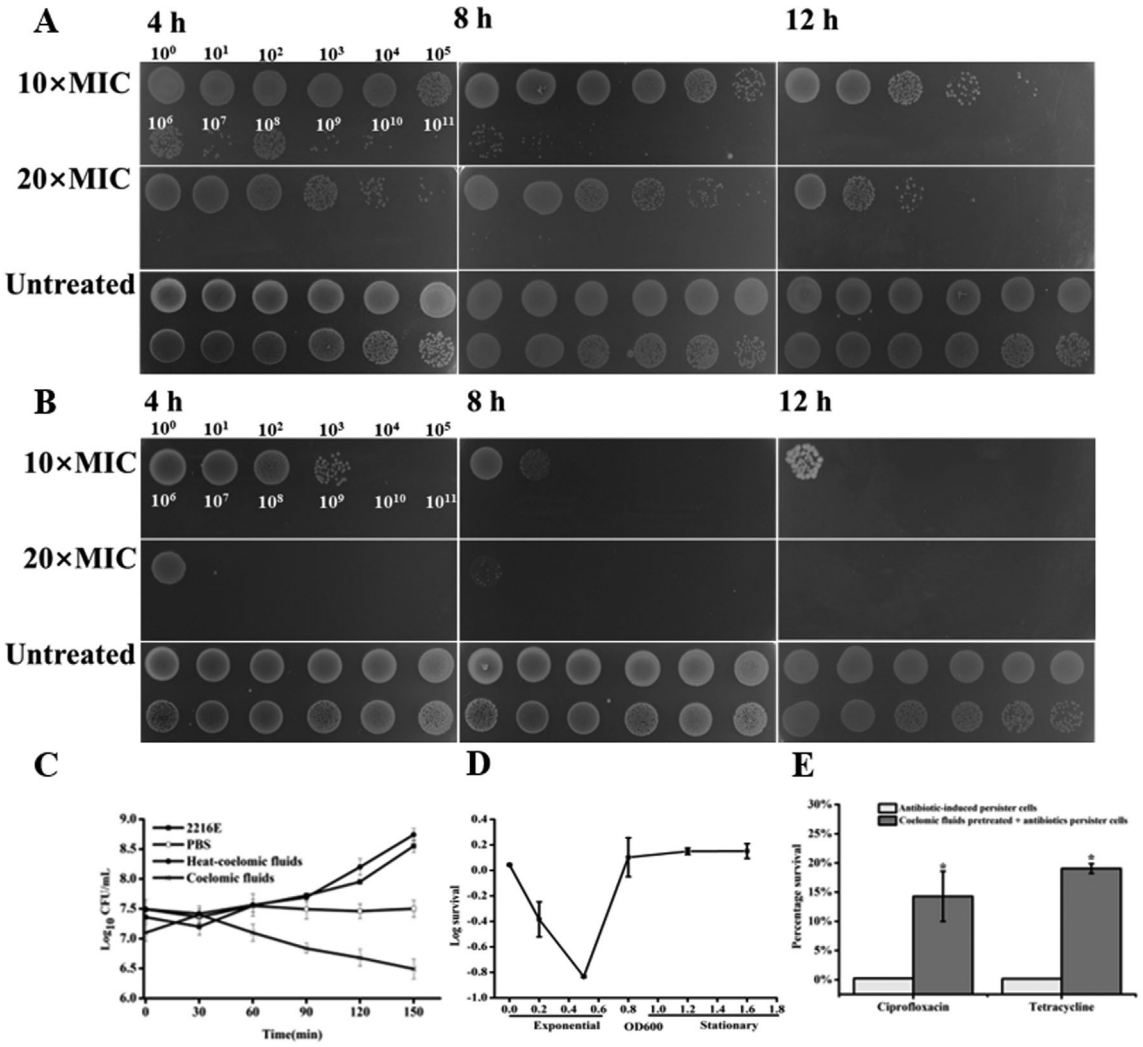


**Fig. 1.** Antibiotic tolerance of *A. japonicus* coelomic fluids-induced persister cells. Exponential-phase cells of *V. splendidus* AJ01 exposed to antibiotics at 10× MIC and 20× MIC.
A. The 125 μg ml$^{-1}$ of ciprofloxacin and 250 μg ml$^{-1}$ of ciprofloxacin for 4, 8, and 12 h at 28°C.
B. The 250 μg ml$^{-1}$ of tetracycline and 500 μg ml$^{-1}$ of tetracycline for 4, 8, and 12 h at 28°C.
C. Exponential-phase cells of *V. splendidus* AJ01 were incubated in fresh 2216E medium, PBS, heat-inactivated coelomic fluids (HCF), or coelomic fluids and grown statically at 28°C without shaking. Colony forming units (CFU) were determined at the indicated time points.
D. The 1 ml suspension of *V. splendidus* AJ01 at different $OD_{600}$ was incubated for 1 h in coelomic fluids, and survival was measured.
E. Coelomic fluids pretreatment increased survival with antibiotics. Statistical significance was determined by Student's *t* test, error bars represent standard errors of three replicates, and **P* value < 0.05.

To characterize the dormancy of the coelomic fluids-induced persister cells, metabolic activity, cellular ATP, ribosome content, and gene expression were examined. We found that the metabolic activity (Fig. 2A and C), cellular ATP level (Fig. 2E) and ribosome content (Fig. 2F) all decreased significantly of the coelomic fluids-induced persister cells compared to the exponential-phase cells. The exponential-phase cells exhibited high metabolic activity, while the coelomic fluid-induced persister cells and antibiotic-induced persister cells had low metabolism similar to the dead cell control (Fig. 2A and C). Only 6% of ciprofloxacin treatment and 1.3% of tetracycline treatment of the coelomic fluids-induced persister cells appeared dead after PI staining (Fig. 2B and D). As control, the dead fraction of exponential-phase cells was 0.19%, and the fraction of dead fraction in the isopropanol-treated dead cell control was 98.9% (Fig. 2B and D). For intracellular ATP levels, the concentration in coelomic fluids-induced persister cells was similar to that of the antibiotic-induced persister cells. For ribosome content, the antibiotic-induced persister cells accumulated a significantly lower level of ribosomes than the exponential-phase cells, and the ribosome content of the persister cells induced by coelomic fluids was also

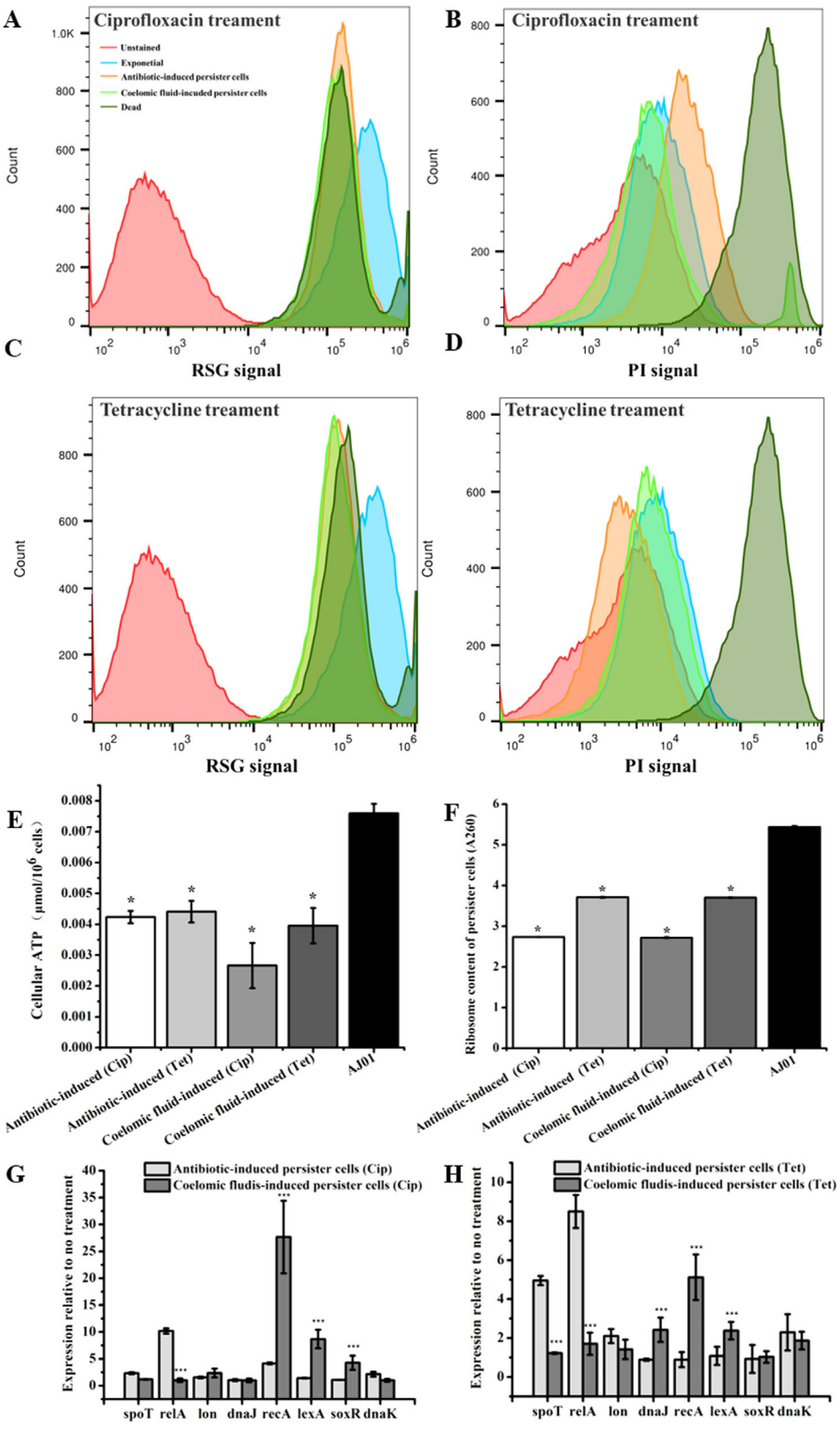


**Fig. 2.** Determination of the metabolic level and gene expression of persister cells. Metabolic activities of exponential-phase cells, antibiotic-induced persister cells, and coelomic fluids-induced persister cells were determined using BacLight RedoxSensor Green (RSG) Vitality kit and flow cytometry.
A and C. Metabolic activity of each cell culture based on the RSG signal.
B and D. Cell viability of each culture based on PI signal. Unstained exponential-phase cells and dead cells (70% isopropanol treatment for 1 h) were used as controls.
E. Cellular ATP level of persister cells. Cellular ATP levels of exponential-phase cells, antibiotic-induced persister cells, and coelomic fluids-induced persister cells were determined using an ATP Content Assay kit.
F. Ribosome content in exponential-phase cells, antibiotic-induced persister cells, and coelomic fluids-induced persister cells.
G. Gene expression in coelomic fluids-induced persister cells (ciprofloxacin treatment) relative to cells without coelomic fluids.
H. Gene expression in coelomic fluids-induced persister cells (tetracycline treatment) relative to cells without coelomic fluids. Statistical significance was determined by Student's *t* test, error bars represent standard errors of three replicates, and **P* value < 0.05.

decreased (Fig. 2F). Moreover, the mRNA transcripts of SOS response and oxidative stress response-related *recA*, *lexA*, and *soxR* genes were significantly upregulated in the coelomic fluids-induced persister cells compared with antibiotic-induced persister cells (Fig. 2G and H). However, the expressions of ppGpp-related *spoT* and *relA* genes were significantly downregulated in the coelomic fluids-induced persister cells (Fig. 2G and H).

To confirm the survived coelomic fluids-induced cells are persister cells, tolerance of the survived cells to multiple classes of antibiotics was tested using a re-grown population from coelomic fluids-induced cells. Ciprofloxacin, tetracycline, ceftriaxone, cefotaxime, ampicillin, and kanamycin were separately added to the persister cell suspension to determine whether the MIC changed. Critically, the MICs for antibiotic-induced persister cells/coelomic fluids-induced persister cells and re-grown population from persister cell population did not change (Supporting Information Tables S3 and S4). Single persister cells also exhibited multidrug tolerance (Fig. 3A and B). The coelomic fluids-induced persister cells and antibiotic-induced persister cells had the same results (data not shown).

Finally, single persister cell resuscitation on agarose gel pads containing a fresh carbon source was investigated after ciprofloxacin treatment and tetracycline treatment, respectively. We found that the coelomic fluids-induced persister cells resuscitate in a manner similar to antibiotic-induced persister cells, in that both had the same morphology of elongated and regular cells (Supporting Information Fig. S3). Together, these findings confirm that the coelomic fluids-induced persister cells are bona fide persister cells.

### *Pathogenicity of persister cells and resuscitated persister cells*

The pathogenicity of coelomic fluids-induced persister cells and resuscitated cells was assayed using seedlings. Using exponential-phase cells as a control, the three kinds of *V. splendidus* AJ01 cells showed distinctively different cumulative survival rates. The *A. japonicus* infected with coelomic fluids-induced persister cells had an obvious decrease in mortality compared with those infected with the exponential-phase cells. The survival rates were 90%, 55%, and 20% in *A. japonicus* seedlings after the challenge with persister cells, exponential-phase cells, and re-grown population from persister cell, respectively. No mortality occurred in the negative control group (Fig. 4A). The *A. japonicus* infected with exponential-phase cells and the re-grown persister population

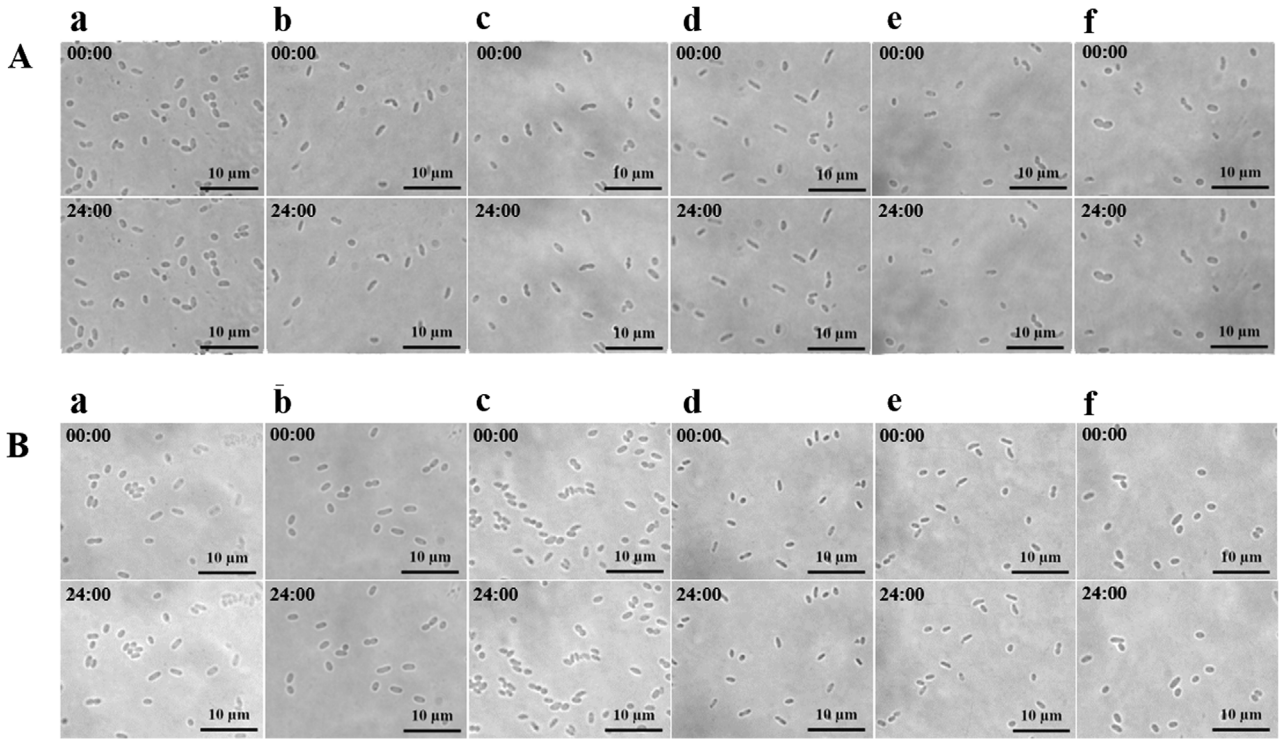


**Fig. 3.** Multidrug tolerance of antibiotic-induced persister cells. Antibiotic-induced persister cells after ciprofloxacin selection (A) or tetracycline selection of persister cells (B) on the 2216E gel pads with the following antibiotic for 24 h: (a) ciprofloxacin, (b) tetracycline, (c) ceftriaxone, (d) cefotaxime, (e) ampicillin, and (f) kanamycin. Cell growth on agarose gel pads was visualized via light microscopy with time points indicated in the upper left side for each panel. Scale bar indicates 10 μm. Three replicates were performed for each sample and a representative sample is shown.

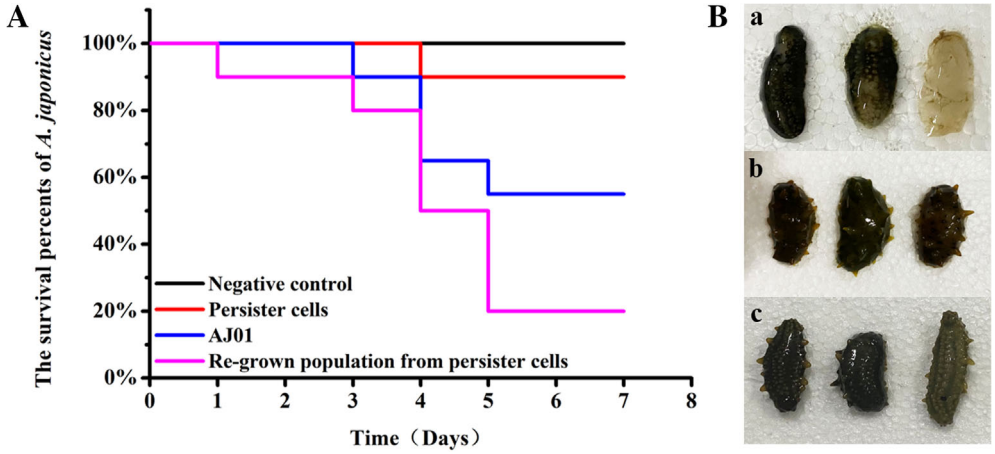


**Fig. 4.** Pathogenicity of re-grown persister cells and persister cells.
A. The survival of *A. japonicus* after challenged with persister cells, re-grown persister cells, and exponential-phase cells. *A. japonicus* without inoculation of bacterial cells was used as negative control.
B. Disease symptoms of *A. japonicus* after bacterial infection. (a) *A. japonicus* after challenged with exponential-phase cells. (b) *A. japonicus* after challenged with re-grown population from persister cell population. (c) Healthy *A. japonicus* from negative control.

exhibited SUS and had skin rot and dissolved body wall (Fig. 4Ba and B**b**). No symptoms of SUS were observed in the *A. japonicus* challenged with the persister cell group and negative control group (Fig. 4Bc). Hence, we found that persister cells had reduced pathogenicity compared to exponential-phase bacteria, but the re-grown population from the persister cells showed higher pathogenicity than the exponential-phase cells. Consistent with the higher virulence, the expression level of the *vsm* gene, encoding a typical pathogenic virulence factor (Le Roux *et al*., 2007; Binesse *et al*., 2008; Liu *et al*., 2016; Zhang *et al*., 2016a), was also higher in re-grown persister cells (Supporting Information Fig. S4).

### *Heterogeneity of single-cell resuscitation*

To corroborate the phenotype of the coelomic fluids-induced persister cells, we observed the resuscitation of single cell on plates with 2216E and compared their morphological phenotypes for exponential-phase cells, antibiotic-induced persister cells, and coelomic fluids-induced persister cells. Dead cells were excluded by PI staining (Supporting Information Fig. S5).

For the exponential-phase cells, cell growth was seen immediately for all cells (Fig. 5A). Cells began to grow in 1 h, and two to three cell divisions were clearly discerned. Microcolonies started to develop on the agarose gel pad after 4 h. However, 1.18% of the single cells also divided slowly, indicating that some slow-growing cells arose randomly under natural culture conditions.

The morphological characteristics of persister cells were initially slightly different from those of the exponential-phase cells, and they produced small colonies (Fig. 5B and C). The resuscitation of 56 single cells was tracked within 6 h via microscopy, and cell division during resuscitation was studied. Cell division was used as the standard to evaluate the resuscitation degree. Different from exponential-phase cells, antibiotic-induced persister cells or coelomic fluids-induced persister cells showed a lag for the first division (Fig. 5D). The single-cell resuscitation rate of antibiotic-induced persister cells after ciprofloxacin treatment was very low. Cell division was delayed, and cells began to wake up after 1 h, and most were awakened slowly compared with normal cells. The resuscitation of antibiotic-induced persister cells from tetracycline treatment was delayed and began to wake at 2 h, and the coelomic fluids-induced persister cells began to wake at 1 h (Fig. 5D). Furthermore, the results clearly show that once cell division occurred, cells recovered immediately to active cells (Fig. 5E). These observations indicated that persister cell resuscitation is heterogeneous and not synchronized (Fig. 5F).

Five phenotypes were observed during single-cell waking (Fig. 6): no growth in 24 h (Fig. 6A), cell elongation and then division (Fig. 6B), cell swelling (Fig. 6C), cell elongation (Figs 6D and S6A), and cell elongation followed by death/disappearance (Fig. 6E). Similar morphological changes were also observed during coelomic fluids-induced persister cells. Most of the persister cells resuscitated by elongating or elongating followed by division (Supporting Information Figs. S6A and S6B).

### *Intracellular dark foci in persister cells*

Under a light microscope, dark foci were observed in the majority of the persister cells. However, no dark foci were observed in exponential-phase cells. These dark foci

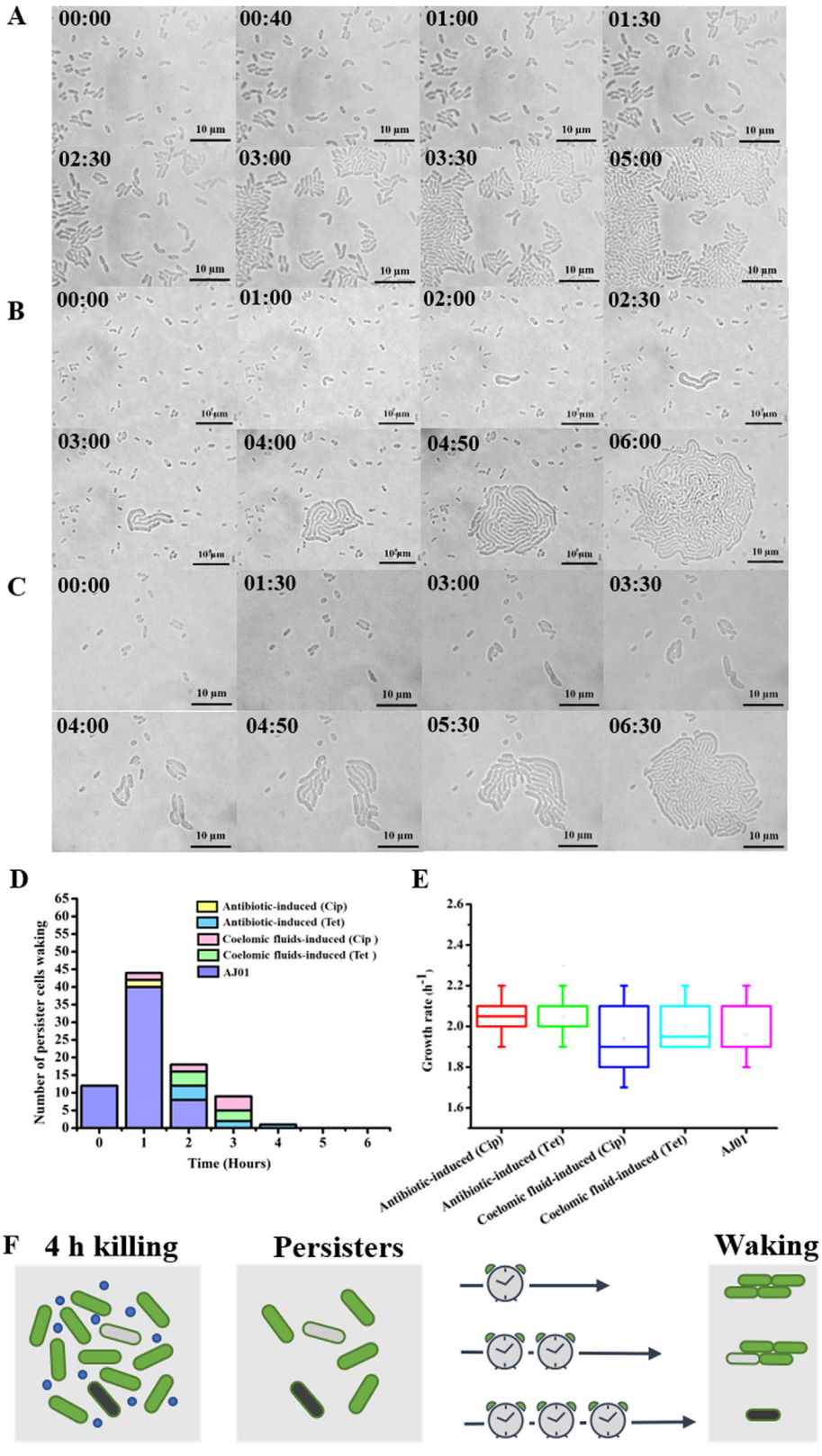


**Fig. 5.** Persister cells waking on agarose gel pads.
A. Exponential-phase cells growing on agarose gel pads. Almost all cells grow immediately by cell division.
B. Antibiotic-induced persister cells after ciprofloxacin selection waking on agarose gel pad.
C. Antibiotic-induced persister cells after tetracycline selection waking on agarose gel pad. Cell growth on agarose gel pads was visualized via light microscopy with time points indicated in the upper left side for each panel.
D. Time course of the number of persister cells and exponential-phase cell waking. We tracked the resuscitation of 56 single-cells within 6 h by microscope, and cell division was used as the standard to evaluate the resuscitation degree.
E. Specific growth rates of exponential-phase cells, and revived antibiotic-induced persister cells, and coelomic fluids-induced persister cells.
F. Schematic diagram illustrating that the persister cell dormancy depth regulates the persister cell waking and growth. Scale bar indicates 10 μm.

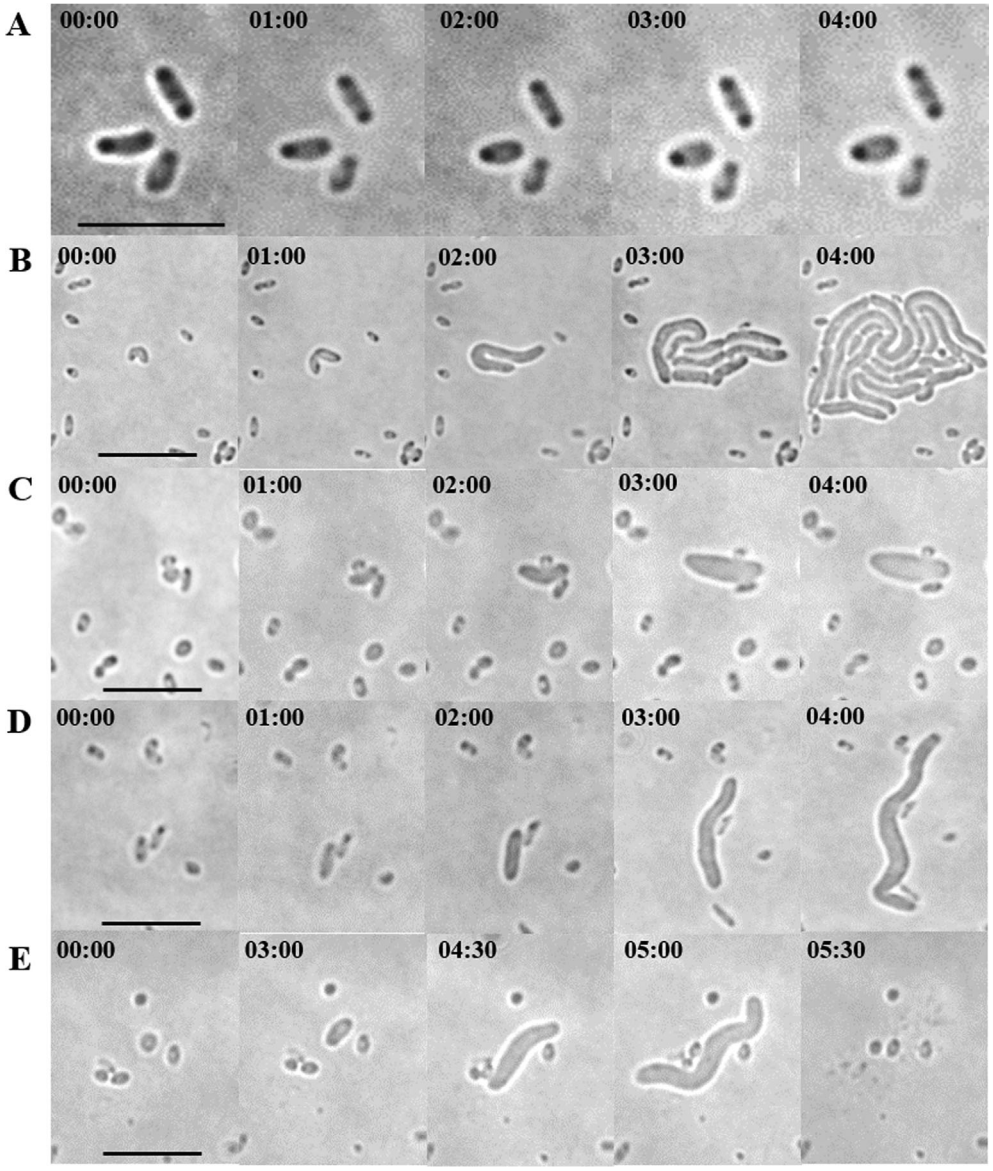


**Fig. 6.** Phenotypic heterogeneity of persister cell waking.
A. Persister cells showing no growth (for up to 24 h).
B. Persister cells gradually elongating then dividing.
C. Persister cells gradually swelling.
D. Persister cells gradually elongating.
E. Persister cells elongating followed by death/disappearance. Cell growth on agarose gel pads was visualized via light microscopy with time points indicated in the upper left side for each panel. Scale bar indicates 10 μm.

were often found in persister cells (ciprofloxacin treatment or tetracycline treatment) and nutrient-depleted cells after prolonged stationary phase incubation for approximately 3 days (Supporting Information Fig. S6Cand S6D). Dark foci were mainly distributed at both ends of the cell poles. Meanwhile, images of the dynamic changes of the dark foci were obtained (Supporting Information Fig. S6C). To test whether the dark foci can cause persister cell dormancy, we attempted to decrease the formation of dark foci by adding chloramphenicol (Fig. 7A) (Siibak *et al*., 2009). Chloramphenicol-treated cells did not show detectable signs of dark foci under bright-field microscopy (Fig. 7B). Consistently, the ratio of persister cells in chloramphenicol-treated cells was significantly higher than that of the antibiotic-induced persister cells after ciprofloxacin treatment (Fig. 7C), confirming that suppression of dark foci can prevent persistence effectively.

Transmission electron microscopy (TEM) and scanning electron microscopy (SEM) were used to explore the

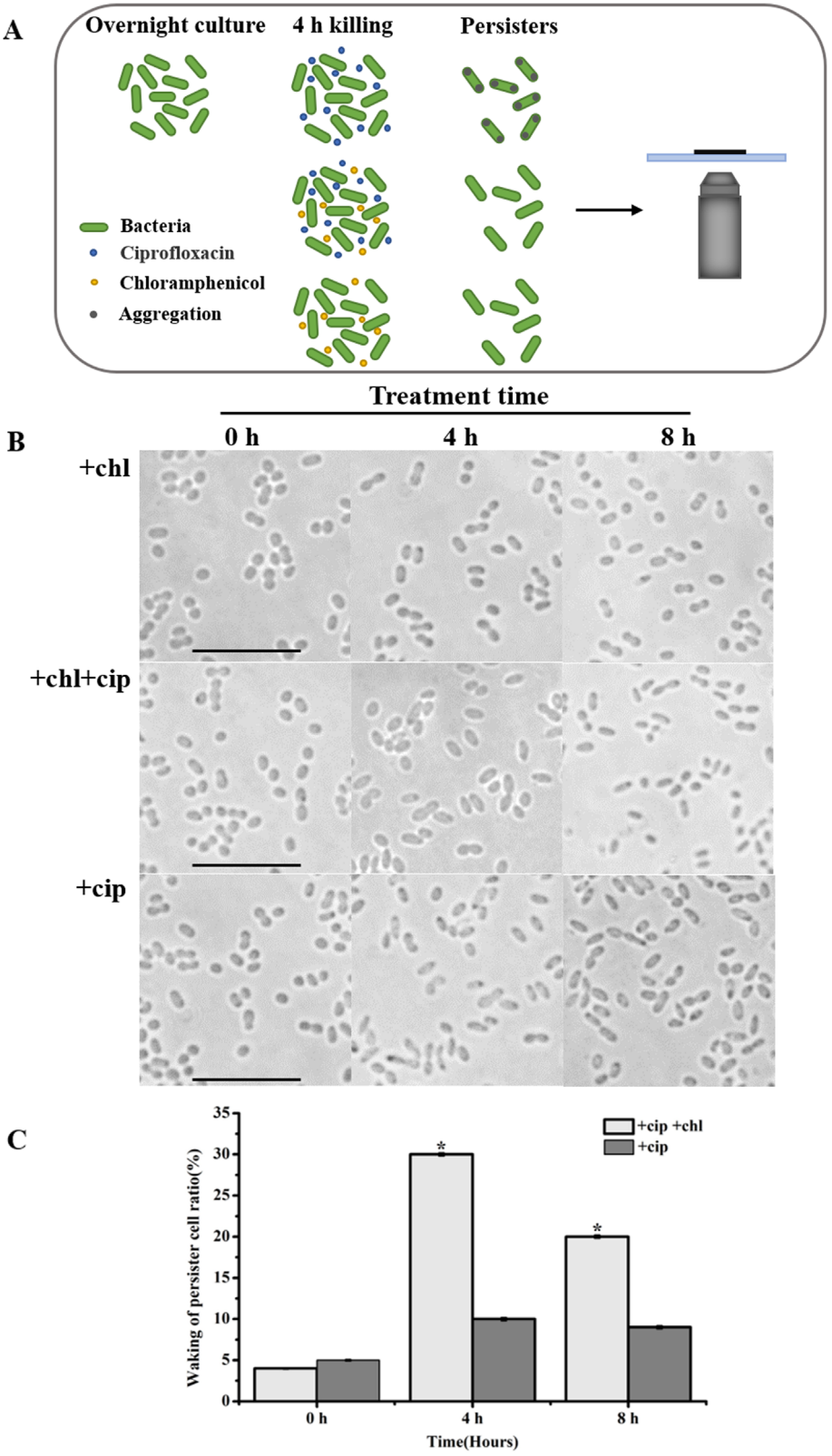


**Fig. 7.** Formation of dark foci correlated with bacterial dormancy.

**A**. Schematic diagram illustrating the prevention cells from dormancy through inhibition of aggresome formation. Overnight cultured cells at 28°C were obtained and divided into three tubes: one aliquot with 125 μg $ml^{-1}$ ciprofloxacin, one aliquot simultaneously with 25 μg $ml^{-1}$ chloramphenicol and 125 μg $ml^{-1}$ ciprofloxacin, the other aliquot with 25 μg $ml^{-1}$ chloramphenicol. The three tubes were further cultured at 28°C for 4 h. A fraction of cells was obtained at the indicated time point, the chloramphenicol and ciprofloxacin washed away, cell morphology was observed under a bright-field microscope, and dormant cell ratio was analysed.

B. The overnight culture cells were treated with or without chloramphenicol for 0, 4, and 8 h. Cell morphology was observed under a bright-field microscope.

C. Waking rate of persister cells with or without chloramphenicol treatment for 0, 4, and 8 h. Waking persister cells are defined as cell resuscitation within 24 h on fresh agarose under a microscope. Statistical significance was determined by Student's *t* test, **P* value < 0.05.

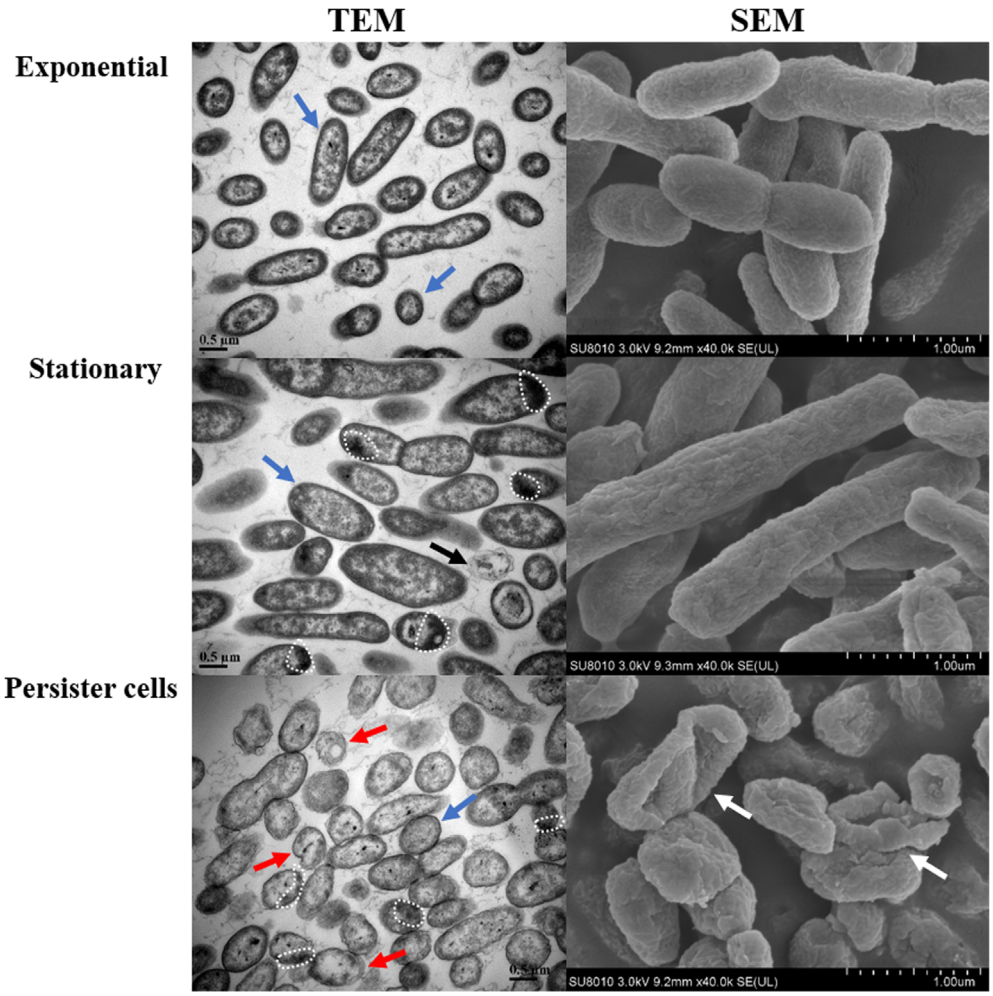


**Fig. 8.** TEM and SEM images of exponential-phase cells, stationary-phase cells, and persister cells. Blue arrows indicate cells with dense cytosol and intact membranes, red arrows indicate cells in the intermediate stage of material loss, black arrows indicate cells with empty cytosol but intact membranes, white arrows indicate cell membrane damage, and white dashed frame indicates that dark foci formed by cytoplasm aggregation, and scale bar of SEM indicates 5000 nm.

morphology between the exponential-phase cells and persister cells. The images confirmed that exponential-phase cells are rod shaped, spherical, and healthy with dense cytosol and cell membrane integrity (Fig. 8). Critically, the majority of the stationary-phase cells are rod shaped, but they also have empty cytosol occasionally (Fig. 8). The results suggest that stationary-phase cells undergo a morphological change as the bacteria progress into the persistent state. Meanwhile, we also observed dark foci by the aggregation of cytoplasm in TEM (Fig. 8) similar to the dark foci observed under the light microscope (Supporting Information Fig. S6D). Antibiotic-induced persister cells and coelomic fluids-induced persister cells contained more spherical cells. These kinds of persister cells are the dense cytosol and empty cytosol types, both of which are injured cells with damaged membranes (Figs 8 and S7).

## Discussion

Whether the coelomic fluids-induced and antibiotic-resistant cells are bona fide persister cells is an important question in our study. In our experiments, we used several experimental methods to characterize persister cells (Kim *et al*., 2018), which have also been validated by 15 independent labs to date (Johnson and Levin, 2013; Kwan *et al*., 2013; Grassi *et al*., 2017; Cui *et al*., 2018; Jin *et al*., 2018; Narayanaswamy *et al*., 2018; Sulaiman *et al*., 2018; Tkhilaishvili *et al*., 2018; Pu *et al*., 2019; Martins *et al*., 2020; Rowe *et al*., 2020; Sun *et al*., 2020; Yu *et al*., 2020; Zhao *et al*., 2020; Zheng *et al*., 2020). These methods are mainly based on the phenotypes of low metabolic activity, high gene expression of ppGpp-pathway related genes, invariable MIC, multidrug tolerance, pathogenicity of re-grown persister cells, and high phenotype

heterogeneity. In the present study, our results demonstrate the presence of antibiotic-induced persister cells in a growing culture of *V. splendidus* AJ01. Additionally, coelomic fluids of *A. japonicus* were shown to induce the formation of persister cells, which are similar to the antibiotic-induced persister cells. Therefore, coelomic fluids-induced persister cells are bona fide persister cells.

The coelomic fluids of *A. japonicus* are a stress factor that pathogens encounter during the bacterial infection process. Coelomic fluids contain important components of the humoral immune system, such as complement and immune factors (Jiang *et al*., 2017; 2020). Our results show that coelomic fluids limit the growth of *V. splendidus* AJ01 (Figs 1C and 1D) and increase bacterial tolerance to antibiotics (Fig. 1F), both of which indicate the formation of persister cells. Putrinš *et al*. (2015) reported that population heterogeneity allows persister cells to survive the combination of antibiotics and human serum. Previous reports indicated that human serum induces formation of persister cells in *V. vulnificus* and *E. coli*. Such findings are consistent with the observation that antagonism occurs when cells are exposed to bactericidal and bacteriostatic antibiotics simultaneously (Ayrapetyan *et al*., 2015a; Pont *et al*., 2020). Moreover, bacteria can survive antibiotic treatments, and persister cells are not eradicated by the immune system of coelomic fluids. For example, *P. aeruginosa* can withstand serum complement-mediated lysis by constructing a group of small variants with some persister-like features (phenotypic heterogeneity) (Pont *et al*., 2020).

Similar to *E. coli* persister cells (Kim *et al*., 2018), the *V. splendidus* persister cells that resuscitated in the presence of nutrients were not synchronized and exhibited five different resuscitation types through single-cell microscopic examination (Fig. 6). Among waking types, cell elongation then division is the most common. Bacterial elongation after antibiotic removal following antibiotic exposure has been demonstrated by many researchers (Chung *et al*., 2009; Yao *et al*., 2012; Kim *et al*., 2018; Maisonneuve *et al*., 2018). Cho *et al*. (2017) reported that cell elongation during revival of persister cells is unique to ciprofloxacin-treated persister cells; however, other studies and our results show that cell elongation is not restricted to the ciprofloxacin-treated persister cells. High levels of ppGpp in tetracycline-, ampicillin-, and rifampicin-induced persister cells are consistent with the coelomic fluids-induced persister cells in our study (Kim *et al*., 2018; Maisonneuve *et al*., 2018). Also, when persister cells begin to divide, they grow with the same doubling time as the exponential-phase cells (Fig. 5) in agreement with Kim *et al*. (2018), who showed that once division begins, the cell is fully recovered. Different times were required for each single persister cell to begin division, indicating the heterogeneity in persister cells (Pu *et al*., 2019). This difference in metabolic level is determined by the ribosome content; cells with high numbers of active ribosomes resuscitate and divide immediately (Kim *et al*., 2018; Wood *et al*., 2019; Song and Wood, 2020). Also, non-resuscitated cells are found if the observation time is restricted to 24 h, and these cells may be viable but nonculturable cells (VBNCs) (Pu *et al*., 2019).

The relationship between the persister cells and VBNCs is disputed. Some researchers consider that VBNCs are viable because the dormant cell shells have intact membranes and are not permeated by the membrane stain propodeum iodide (PI) (Dong *et al*., 2020). In contrast, some researchers consider that persister cells and VBNCs share many common features, so they conclude that viable fraction of the VBNC population and persister cells describe the same dormant phenotype, and the non-resuscitating fraction of VBNCs is dead cells (Kim *et al*., 2018). In our present study, we observed five phenotypes during persister single-cell waking, of which there are cells that showed no growth after 24 h (Fig. 6A), and resuscitation still did not occur when the observation time increased, which is evidence for the presence of dead cells (i.e., VBNCs), after antibiotic treatment. In another experiment here, the persister cells were observed by TEM, and there are a few cells showing spheroid, hollow, empty cytosol and membrane-enclosed vessels (Fig. 8). This is the second line of evidence for the presence of dead cells (i.e., VBNCs) (Kim *et al*., 2018; Wood *et al*., 2019; Song and Wood, 2021). Thus, it can be concluded that the coelomic fluids of *A. japonicus* induce the formation of both persister cells and dead VBNCs, mainly based on the single-cell observation under microscopy.

We found that most persister cells and prolonged stationary-phase cells had empty cytosol and dark foci. The loss of cell content fits well with the fact that *Salmonella typhi* persister cells shrink and become spherical (Zeng *et al*., 2013). In a previous report, Pu *et al*. (2019) found that dark foci comprise a wide collection of intracellular protein aggregates. This structure is only formed in no growing bacterial cells, and the structure depolymerize to recruit multiple key proteins when the cell recovers to growth. The dark foci are similar to the regrowth-delay body described by Yu *et al*. (Yu *et al*., 2019). Our results confirm that the suppression of dark foci can prevent cell persistence effectively (Fig. 7). Hence, the dark foci can be used as an indicator of dormancy in *V. splendidus* AJ01 and can be seen as a marker of persister cells.

Persister cells have a role in the relapse and recalcitrance of infections (Fisher *et al*., 2017). Their importance may be deduced from the fact that persister cells in *P. aeruginosa*, *M. tuberculosis*, *S. aureus* and *S. typhi* play important roles in disease (Möker *et al*., 2010;

Fauvart *et al*., 2011; Dhillon *et al*., 2014; Bakkeren *et al*., 2019; Yee *et al*., 2019). Also, Putrinš *et al*. (2015) reported that persister cells with phenotypic heterogeneity enabled uropathogenic *E. coli* to evade killing by antibiotics and serum complement. In addition, some of the heat-labile factors in human serum, such as complement, may induce persistence (Ayrapetyan *et al*., 2015b). In our present study, in the presence of *A. japonicus* coelomic fluids, the active cells of *V. splendidus* AJ01 enter into the persister state and the cells survive the host immune responses with low virulence to *A. japonicus*. The immune factors in *A. japonicus* coelomic fluids may be the factors that induce *V. splendidus* AJ01 persistence. Together, these results indicate that persister cells may play a role in the natural infection of the *A. japonicus*, which needs to be studied in more detail.

In conclusion, persister cells exist in the cultured population of *V. splendidus* AJ01, but they are induced 100-fold by *A. japonicus* coelomic fluids. The coelomic fluids-induced persister cells behave the same as antibiotic-induced persister cells in terms of multiple antibiotic tolerance and low metabolic activity. The resuscitation of coelomic fluids-induced persister cells exhibits high phenotypic heterogeneity, and five types are present: no growth, expansion, elongation, elongation and then division, and elongation followed by death/disappearance. Moreover, dark foci are present in both the coelomic fluids-induced persister cells and the antibiotic-induced persister cells. The molecular mechanism through which coelomic fluids induce persister cell formation and resuscitation will be elucidated in further studies.

## Experimental procedures

### *Bacterial strains and culture conditions*

*Vibrio splendidus* AJ01 used in this study was isolated from a diseased sea cucumber (*A. japonicus*) from a Jinzhou hatchery. The bacterium was identified by 16S rDNA sequence analysis, and its pathogenicity was determined in our previous study (Zhang *et al*., 2016b). The strain was cultured at 28°C in 2216E medium (5 $g \cdot l^{-1}$ tryptone, 1 $g \cdot l^{-1}$ yeast extract, and 0.01 $g \cdot l^{-1}$ $FePO_4$ in filtered natural seawater).

### *Minimum inhibitory concentration and antibiotic tolerance*

MICs were measured as described previously (Zhang *et al*., 2019) with ciprofloxacin, tetracycline, ceftriaxone, cefotaxime, ampicillin, and kanamycin. To assay antibiotic tolerance, *V. splendidus* AJ01 was inoculated into 2216E medium at a ratio of 1:100 and grown overnight. Ciprofloxacin and tetracycline were added at 10× MIC and 20× MIC, and the cultures were maintained at 28°C with shaking to 12 h, then, 1 ml of the cell culture was washed and diluted serially by phosphate buffer saline (PBS), and 10 μl of samples were spotted onto 2216E agar plates; colonies were counted after overnight incubation at 28°C. Bacterial cultures that are not treated with antibiotics were used as controls.

### *Antibiotic-induced persister cells*

Antibiotic-induced persister cells were selected as described by Li and Zhang (2007). Overnight cultures of *V. splendidus* AJ01 were inoculated into 50 ml of 2216E and cultured overnight. Thereafter, 10× MIC was chosen to minimize the survival of potential spontaneous resistant mutants: 125 $\mu g \cdot ml^{-1}$ ciprofloxacin or 250 $\mu g \cdot ml^{-1}$ tetracycline was added separately to the cultures and treated for 4 h at 28°C to eradicate the non-persister cells. One millilitre of the cell culture was washed and diluted serially by PBS, and 10 μl of samples were spotted onto 2216E agar plates; colonies were counted after overnight incubation at 28°C.

### *Coelomic fluids-induced persister cells*

In brief, *A. japonicus* were dissected on ice using sterilized scissors, and coelomic fluids were filtered through a 200 Mesh Cell Cribble to remove large tissue debris. The fluids were then centrifuged at 800*g* at 16°C for 10 min. Exponential-phase cells of *V. splendidus* AJ01 were washed twice with PBS and resuspended in 1 ml of the coelomic fluids. These suspensions were incubated at 16°C for 1 h. Then, coelomic fluids were washed, and antibiotic was added at a final concentration of 10× MIC. Cultures were incubated at 28°C for another 4 h. Cells were then washed three times to remove the antibiotic, and the coelomic fluids-induced persister cells were obtained.

### *Metabolic activity of persister cells*

Metabolic activity was measured through a BacLight™ RedoxSensor™ Green Vitality kit (Thermo Fisher Scientific, Waltham, MA, USA) following the manufacturer's instructions. The metabolic activity of exponential-phase cells and persister cells was measured by flow cytometry (Beckman Coulter, USA) by pelleting cells and washing twice with PBS. For the negative control (dead cells), 1 ml of exponential-phase cells was centrifuged, resuspended in 70% isopropanol, and incubated for 1 h at room temperature. Propodeum iodide and redox sensor stains were used with samples incubated at 28°C for 10 min with light protection. The fluorescence signal was

analysed by flow cytometry using the FL1 (520 nm) and FL3 (620 nm) channels.

### *Cellular ATP measurement*

Cellular ATP was measured using an ATP Content Assay kit (Solarbio, Beijing, China) following the manufacturer's instructions. Cells were collected at approximately $5 \times 10^6$ CFU·ml$^{-1}$ before the experiment. Cells were subjected to ultrasonic disruption and centrifugation at 10 000*g* for 10 min at 4°C, and the supernatant was added with 500 μl of chloroform and centrifuged at 10 000*g* for 3 min at 4°C. The supernatant was collected, and cellular ATP was measured according to the kit's instructions. The absorbance at 340 nm was measured using a microplate reader.

### *Ribosome measurement*

Ribosomes were measured through a Bacterial Ribosome Extraction kit (LMAI-BIO, Shanghai, China) following the manufacturer's instructions. Briefly, buffer A and buffer B were added to 500 mg wet weight of each bacterium and mixed well on ice for 30 min. Cells were disrupted by a French press at 16 000 psi twice, then treated with 5 U of DNase I (RNase-free) on ice for 10 min. The pellet was discarded, and supernatants were collected by centrifugation at 1000*g* for 5 min followed by centrifugation at 170 000*g* for 60 min, and 400 μl of buffer C was added to the precipitate and centrifuged at 170 000*g* for 60 min. The ribosome pellets were resuspended in PBS, and the RNA in ribosomes was quantified at $A_{260}$.

### *Single-cell resuscitation on agarose gel pads*

Resuscitation of single persister cells was performed on an agarose gel pads (Zhang *et al*., 2019). Three kinds of solid agar, including 2216E medium without carbon source, 2216E medium containing specific antibiotic, and 2216E medium containing carbon source, were prepared using the sandwich method (Kim *et al*., 2018). Briefly, 1.5% of low-melting agarose was added to 2216E liquid medium and melted by microwaving. Single-cell resuscitation was observed under a light microscope (ZEISS) maintained at 28°C. Single-cell resuscitation in the presence of different antibiotics was performed using the agarose gel pads containing each antibiotic of ciprofloxacin, tetracycline, ceftriaxone, cefotaxime, ampicillin, and kanamycin, and the concentration of antibiotic was 10× MIC.

### *Quantitative real-time reverse transcriptase -PCR analysis*

Total RNA was isolated from exponential-phase cells and persister cells using a Bacterial RNA Isolation kit (Omega, Norcross, USA). The purity and quantity of the total RNA were determined using a Nano Drop™ 2000 spectrophotometer (Thermo Fisher Scientific). cDNA was synthesized using a Primescript™ 1st cDNA Synthesis kit (Takara, Beijing, China). Qutantitative real-time reverse transcriptase -PCR was performed in an ABI 7500 real-time detection system (Applied Biosystems) using a SYBR ExScript RT-PCR kit (Takara, Beijing, China). Amplifications were performed in a 20 μl of reaction volume containing 8 μl of diluted cDNA, 1 μl of each primer, and 10 μl of SYBR Green Mix (Takara). The reaction mixture was incubated for 5 min at 95°C followed by 40 amplification cycles of 15 s at 95°C, 20 s at 60°C, and 20 s at 72°C. The $2^{-\triangle\triangle CT}$ method was used to analyse the expression level of each gene. Primers used for qutantitative real-time reverse transcriptase-PCR are listed in the Supporting Information Table S1, and the primers used for the reference control of 16S rDNA were 933F and 16SRTR1. Statistical analyses were performed using the two-tailed Student's t test.

### *Experimental infection*

Healthy *A. japonicus* seedlings (weight 3.2 ± 1.1 g, size range 2.2–3.6 cm) was purchased from Hai Deli Sea Products (Qingdao, China). They specimens were acclimatized in 100 l tanks supplied with aerated, filtered sea water maintained at 16°C and salinity of approximately 30 ppt. Seawater was changed daily during the acclimation period of 5 days. Then, *A. japonicus* were randomly divided into four tanks with each containing 20 individuals. The first group was infected with *V. splendidus* AJ01 at a final concentration of $1.0 \times 10^7$ CFU·ml$^{-1}$. The second group was infected with antibiotic-induced persister cells from ciprofloxacin treatment at the same concentration. The third group was infected with re-grown population from the antibiotic-induced persister cells at the same concentration. The last group without bacterial inoculation was used as the negative control. The tanks were checked at approximately an interval of 24 h, and dead *A. japonicus* were removed. *A. japonicus* seedlings with skin ulceration and detached from the surface of tanks was considered dead.

### *Transmission electron microscopy and scanning electron microscopy imaging*

For the TEM assays, one milliliter of exponential-phase cells, stationary-phase cells, and persister cells were

pelleted by centrifugation at 5000*g* for 5 min, washed twice with PBS, and resuspended in 1 ml of 2.5% glutaric dialdehyde. First, cells were fixed with 2.5% (v/v) glutaraldehyde in 0.1 M sodium cacodyl ate buffer. Pellets were washed three times with 0.1 M sodium cacodyl ate followed by secondary fixation with 1% osmium tetroxide. Next, samples were washed three times with 0.1 M sodium cacodyl ate and water followed by staining with 2% uranyl acetate. Samples were then dehydrated in a graded series of ethanol (70%, 85%, 95%, and $3 \times 100\%$), washed three times with acetone, embedded, and polymerized at 65°C overnight. Ultrathin sections 70 nm in size were cut and stained in uranyl acetate followed by lead citrate. Sample grids were examined using a Hitachi H-7650 transmission electron microscope at 200 kV.

For the SEM assays, one milliliter of sample was washed twice with PBS and fixed with 2.5% (v/v) precooling glutaraldehyde at room temperature in a dark place. Thereafter, samples were washed three times with PBS, fixed with 1% $OsO_4$ for 1 h and washed three times in phosphate buffer. The specimens were dehydrated with an increasing ethyl alcohol gradient of 15%, 30%, 50%, 70%, 80%, 90%, 95%, and 100% (v/v) with each step. Finally, it was dried overnight and gilt in time. The dehydrated sample was coated with platinum-palladium and observed under a Hitachi Model SU8010FE scanning electron microscope at 15 kV.

## Acknowledgements

This work was financially supported by the Zhejiang Provincial Natural Science Foundation (LR20C190001, LZ19C190001), and the K.C. Wong Magna Fund at Ningbo University.

## References

Ayrapetyan, M., Williams, T.C., and Oliver, J.D. (2015a) Bridging the gap between viable but non-culturable and antibiotic persistent bacteria. *Trends Microbiol* **23**: 7–13.

Ayrapetyan, M., Williams, T.C., Baxter, R., and Oliver, J.D. (2015b) Viable but nonculturable and persister cells coexist stochastically and are induced by human serum. *Infect Immun* **83**: 4194–4203.

Bakkeren, E., Huisman, J.S., Fattinger, S.A., Hausmann, A., Furter, M., Egli, A., *et al*. (2019) *Salmonella* persisters promote the spread of antibiotic resistance plasmids in the gut. *Nature* **573**: 276–280.

Balaban, N.Q. (2011) Persistence: mechanisms for triggering and enhancing phenotypic variability. *Curr Opin Genet Dev* **21**: 768–775.

Binesse, J., Delsert, C., Saulnier, D., Champomier-Verges, M.C., Zagorec, M., Munier-Lehmann, H., *et al*. (2008) Metalloprotease*Vsm* is the major determinant of toxicity for extracellular products of *Vibrio splendidus*. *Appl Environ Microbiol* **74**: 7108–7117.

Bui, L.M., Conlon, B.P., and Kidd, S.P. (2017) Antibiotic tolerance and the alternative lifestyles of *Staphylococcus aureus*. *Essays Biochem* **61**: 71–79.

Cao, R., Wang, Q., Yang, D., Liu, Y., Ran, W., Qu, Y., *et al*. (2018) $CO_2$-induced ocean acidification impairs the immune function of the *Pacific oyster* against *Vibrio splendidus* challenge: an integrated study from a cellular and proteomic perspective. *Sci Total Environ* **625**: 1574–1583.

Cho, J., Carr, A.N., Whitworth, L., Johnson, B., and Wilson, K.S. (2017) MazEF toxin-antitoxin proteins alter *Escherichia coli* cell morphology and infrastructure during persister formation and regrowth. *Microbiology (Reading)* **163**: 308–321.

Chung, H.S., Yao, Z., Goehring, N.W., Kishony, R., Beckwith, J., and Kahne, D. (2009) Rapid beta-lactam-induced lysis requires successful assembly of the cell division machinery. *Proc Natl Acad Sci U S A* **106**: 21872–21877.

Cui, P., Niu, H., Shi, W., Zhang, S., Zhang, W., and Ying, Z. (2018) Identification of genes involved in bacteriostatic antibiotic-induced persister formation. *Front Microbiol* **9**: 413.

Dhillon, J., Fourie, P.B., and Mitchison, D.A. (2014) Persister populations of *mycobacterium tuberculosis* in sputum that grow in liquid but not on solid culture media. *J Antimicrob Chemother* **69**: 437–440.

Dong, K., Pan, H., Yang, D., Rao, L., Zhao, L., Wang, Y., *et al.* (2020) Induction, detection, formation, and resuscitation of viable but non-culturable state microorganisms. *Compr Rev Food Sci Food Saf*, **19**: 149–183.

Fauvart, M., de Groote, V.N., and Michiels, J. (2011) Role of persister cells in chronic infections: clinical relevance and perspectives on anti-persister therapies. *J Med Microbiol* **60**: 699–709.

Fisher, R.A., Gollan, B., and Helaine, S. (2017) Persistent bacterial infections and persister cells. *Nat Rev Microbiol* **15**: 453–464.

Goormaghtigh, F., Fraikin, N., Putrinš, M., Hallaert, T., Hauryliuk, V., Garcia-Pino, A., *et al*. (2018) Reassessing the role of type ii toxin-antitoxin systems in formation of *Escherichia coli* type ii persister cells. *mBio* **9**: e00640–e00618.

González, R., Brokordt, K., Cárcamo, C.B., Coba, T., Oyanedel, D., Mercado, L., *et al*. (2017) Molecular characterization and protein localization of the antimicrobial peptide big defensin from the scallop *Argopecten purpuratus* after *Vibrio splendidus* challenge. *Fish Shellfish Immunol* **68**: 173–179.

Grassi, L., Di Luca, M., Maisetta, G., Rinaldi, A.C., Esin, S., Trampuz, A., and Batoni, G. (2017) Generation of persister cells of *Pseudomonas aeruginosa* and *Staphylococcus aureus* by chemical treatment and evaluation of their susceptibility to membrane-targeting agents. *Front Microbiol* **8**: 1917.

Helaine, S., Cheverton, A.M., Watson, K.G., Faure, L.M., Matthews, S.A., and Holden, D.W. (2014) Internalization of *salmonella* by *macrophages* induces formation of nonreplicating persisters. *Science* **343**: 204–208.

Huq, A., Whitehouse, C.A., Grim, C.J., Alam, M., and Colwell, R.R. (2008) Biofilms in water, its role and impact in human disease transmission. *Curr Opin Biotechnol* **19**: 244–247.

Jiang, J., Zhao, Z., Pan, Y., Dong, Y., Gao, S., Jiang, B., *et al*. (2020) Proteomics reveals the gender differences in humoral immunity and physiological characteristics associated with reproduction in the sea cucumber *Apostichopus japonicus*. *J Proteomics* **217**: 103687.

Jiang, J., Zhou, Z., Dong, Y., Zhao, Z., Sun, H., Wang, B., *et al*. (2017) Comparative expression analysis of immune-related factors in the sea cucumber *Apostichopus japonicus*. *Fish Shellfish Immunol* **72**: 342–347.

Jin, X., Kightlinger, W., Kwon, Y.-C., and Hong, S.H. (2018) Rapid production and characterization of antimicrobial colicins using *Escherichia coli*-based cell-free protein synthesis. *Synthetic Biology* **3**: ysy004.

Johnson, P.J.T., and Levin, B.R. (2013) Pharmacodynamics, population dynamics, and the evolution of persistence in *Staphylococcus aureus*. *PLoS Genet* **9**: e1003123.

Kim, J.S., Yamasaki, R., Song, S., Zhang, W., and Wood, T. K. (2018) Single cell observations show persister cells wake based on ribosome content. *Environ Microbiol* **20**: 2085–2098.

Kwan, B.W., Valenta, J.A., Benedik, M.J., and Wood, T.K. (2013) Arrested protein synthesis increases persister-like cell formation. *Antimicrob Agents Chemother* **57**: 1468–1473.

Le, R.F., Binesse, J., Saulnier, D., and Mazel, D. (2007) Constructionof a *Vibrio splendidus* mutant lacking the metalloprotease gene *vsm* by use of a novel counter-selectable suicide vector. *Appl Environ Microbiol* **73**: 777–784.

Lewis, K. (2005) Persister cells and the riddle of biofilm survival. *Biochemistry (Mosc)* **70**: 267–274.

Li, Y., and Zhang, Y. (2007) PhoU is a persistence switch involved in persister formation and tolerance to multiple antibiotics and stresses in *Escherichia coli*. *Antimicrob Agents Chemother* **51**: 2092–2099.

Liu, H., Zheng, F., Sun, X., Hong, X., Dong, S., Wang, B., *et al*. (2010) Identification of the pathogens associated with skin ulceration and peristome tumescence in cultured sea cucumbers *Apostichopus japonicus* (Selenka). *J Invertebr Pathol* **105**: 236–242.

Liu, R., Chen, H., Zhang, R., Zhou, Z., Hou, Z.H., Gao, D.H., *et al*. (2016) The comparative transcriptome analysis of *Vibrio splendidus* Z6 revealed the mechanism of its pathogenicity at low temperature. *Appl Environ Microbiol* **82**: 2050–2061.

Long, Y., Fu, W., Li, S., Ren, H., Li, M., Liu, C., *et al*. (2019) Identification of novel genes that promote persister formation by repressing transcription and cell division in *Pseudomonas aeruginosa*. *J Antimicrob Chemother* **74**: 2575–2587.

Maisonneuve, E., and Gerdes, K. (2014) Molecular mechanisms underlying bacterial persisters. *Cell* **157**: 539–548.

Maisonneuve, E., Castro-Camargo, M., and Gerdes, K. (2018) (p)ppGpp controls bacterial persistence by stochastic induction of toxin-antitoxin activity. *Cell* **172**: 1135.

Martins, D., McKay, G.A., English, A.M., and Nguyen, D. (2020) Sublethal paraquat confers multidrug tolerance in *Pseudomonas aeruginosa* by inducing superoxide dismutase activity and lowering envelope permeability. *Front Microbiol* **11**: 576708.

Michiels, J.E., van den Bergh, B., Verstraeten, N., and Michiels, J. (2016) Molecular mechanisms and clinical implications of bacterial persistence. *Drug Resist Updat* **29**: 76–89.

Möker, N., Dean, C.R., and Tao, J. (2010) *Pseudomonas aeruginosa* increases formation of multidrug-tolerant persister cells in response to quorum-sensing signaling molecules. *J Bacteriol* **192**: 1946–1955.

Narayanaswamy, V.P., Keagy, L.L., Duris, K., Wiesmann, W., Loughran, A.J., Townsend, S.M., *et al*. (2018) Novel glycopolymer eradicates antibiotic- and CCCP-induced persistercells in *Pseudomonas aeruginosa*. *Front Microbiol* **9**: 1724.

Pont, S., Fraikin, N., Caspar, Y., Van, M.L., Attrée, I., and Cretin, F. (2020) Bacterial behavior in human blood reveals complement evaders with some persister-like features. *PLoS Pathog* **16**: e1008893.

Pu, Y., Li, Y., Jin, X., Tian, T., Ma, Q., Zhao, Z.Y., *et al*. (2019) ATP-dependent dynamic protein aggregation regulates bacterial dormancy depth critical for antibiotic tolerance. *Mol Cell* **73**: 143, e4–156.

Putrinš, M., Kogermann, K., Lukk, E., Lippus, M., Varik, V., Tenson, T., *et al*. (2015) Phenotypic heterogeneity enables uropathogenic *Escherichia coli* to evade killing by antibiotics and serum complement. *Infect Immun* **83**: 1056–1067.

Yee, R., Yuting, Y., Shi, W., Brayton, C., Tarff, A., Fen, J., *et al*. (2019) Infection with persister forms of *Staphylococcus aureus* causes a persistent skin infection with more severe lesions in mice: failure to clear the infection by the current standard of care treatment. *Discov Med* **28**: 7–16.

Rowe, S.E., Wagner, N.J., Li, L., Beam, J.E., Wilkinson, A. D., Radlinski, L.C., *et al*. (2020) Reactive oxygen species induce antibiotic tolerance during systemic *Staphylococcus aureus* infection. *Nat Microbiol* **5**: 282–290.

Sanders, C.C. (1988) Ciprofloxacin: in vitro activity, mechanism of action, and resistance. *Rev Infect Dis* **10**: 516–527.

Siibak, T., Peil, L., Xiong, L., Mankin, A., and Tenson, T. (2009) Erythromycin-and chloramphenicol-induced ribosomal assembly defects are secondary effects of protein synthesis inhibition. *Antimicrob Agents Chemother* **53**: 563–571.

Silva-Valenzuela, C.A., Lazinski, D.W., Kahne, S.C., Nguyen, Y., Molina-Quiroz, R.C., and Camilli, A. (2017) Growth arrest and a persister state enable resistance to osmotic shock and facilitate dissemination of *Vibrio cholerae*. *ISME J* **11**: 2718–2728.

Skurnik, D., Roux, D., Cattoir, V., Da Nilchanka, O., Lu, X., Yoder-Himes, D.R., *et al*. (2013) Enhanced in vivo fitness of carbapenem-resistant oprD mutants of *Pseudomonas aeruginosa* revealed through high-throughput sequencing. *Proc Natl Acad Sci U S A* **110**: 20747–20752.

Song, S., and Wood, T.K. (2021) 'Viable but non-culturable cells' are dead. *Environ Microbiol* **23**: 2335–2338.

Song, S., and Wood, T.K. (2020) ppGpp ribosome dimerization model for bacterial persister formation and resuscitation. *Biochem Biophys Res Commun* **523**: 281–286.

Stapels, D.,.A.C., Hill, P.,.W.S., Westermann, A.J., Fisher, R.,.A., Thurston, T.,.L., Saliba, A.-E., *et al*. (2018) *Salmonella* persisters undermine host immune defenses during antibiotic treatment. *Science* **362**: 1156–1160.

Sulaiman, J.E., Hao, C., and Lam, H. (2018) Specific enrichment and proteomics analysis of *Escherichia coli* persisters from rifampin pretreatment. *J Proteome Res* **17**: 3984–3996.

Sun, F., Bian, M., Li, Z., Lv, B., Gao, Y., Wang, Y., and Fu, X. (2020) 5-methylindole potentiates aminoglycoside against gram-positive bacteria including *Staphylococcus aureus* persisters under hypoionic conditions. *Front Cell Infect Microbiol* **10**: 84.

Thomson, R., Macpherson, H.L., Riaza, A., and Birkbeck, T. H. (2005) *Vibrio splendidus* biotype 1 as a cause of mortalities in hatchery-reared larval turbot, *Scophthalmus maximus* (L.). *J Appl Microbiol* **99**: 243–250.

Tkhilaishvili, T., Lombardi, L., Klatt, A.-B., Trampuz, A., and Di, L.M. (2018) Bacteriophage Sb-1 enhances antibiotic activity against biofilm, degrades exopolysaccharide matrix and targets persisters of *Staphylococcus aureus*. *Int J Antimicrob Agents* **52**: 842–853.

Toprak, E., Veres, A., Michel, J.-B., Chait, R., Hartl, D.L., and Roy, K. (2011) Evolutionary paths to antibiotic resistance under dynamically sustained drug selection. *Nat Genet* **44**: 101–105.

Torresi, M., Acciari, V.A., Piano, A., Serratore, P., Prencipe, V., and Migliorati, G. (2011) Detection of *Vibrio splendidus* and related species in *Chamelea gallina* sampled in the adriatic along the abruzzi coastline. *Vet Ital* **47**: 363–370.

The VibrioSea Consortium, Vezzulli, L., Pezzati, E., Moreno, M., Fabiano, M., Pane, L., and Pruzzo, C. (2009) Benthic ecology of *vibrio spp*. and pathogenic *vibrio* species in a coastal mediterranean environment (La Spezia gulf, Italy). *Microb Ecol* **58**: 808–818.

Wilmaerts, D., Windels, E.M., Verstraeten, N., and Michiels, J. (2019) General mechanisms leading to persister formation and awakening. *Trends Genet* **35**: 401–411.

Wood, T.K., Song, S., and Yamasaki, R. (2019) Ribosome dependence of persister cell formation and resuscitation. *J Microbiol* **57**: 213–219.

Yao, Z., Kahne, D., and Kishony, R. (2012) Distinct single-cell morphological dynamics under beta-lactam antibiotics. *Mol Cell* **48**: 705–712.

Yu, J., Yang, L., Yin, H., and Chang, Z. (2019) Regrowth-delay body as a bacterial subcellular structure marking multidrug-tolerant persisters. *Cell Discov* **5**: 8.

Yu, W., Li, D., Li, H., Tang, Y., Tang, H., Ma, X., *et al*. (2020) Absence of tmRNA increases the persistence to cefotaxime and the intercellular accumulation of metabolite glcNAc in *Aeromonas veronii*. *Front Cell Infect Microbiol* **10**: 44.

Zeng, B., Zhao, G., Cao, X., Yang, Z., Wang, C., and Hou, L. (2013) Formation and resuscitation of viable but nonculturable *Salmonella typhi*. *Biomed Res Int* **2013**: 907170.

Zhang, C., Liang, W., Zhang, W., and Li, C. (2016a) Characterization of a metalloprotease involved in *Vibrio splendidus* infection in the sea cucumber, *Apostichopus japonicus*. *Microb Pathog* **101**: 96–103.

Zhang, W., Li, C. (2021). Virulence mechanisms of vibrios belonging to the Splendidus clade as aquaculture pathogens, from case studies and genome data. *Reviews in Aquaculture*. http://dx.doi.org/10.1111/raq.12555

Zhang, W., Liang, W., and Li, C. (2016b) Inhibition of marine *Vibrio spp*. by pyoverdine from *Pseudomonas aeruginosa* PA1. *J Hazard Mater* **302**: 217–224.

Zhang, W., Yamasaki, R., Song, S., and Wood, T.K. (2019) Interkingdom signal indole inhibits *Pseudomonas aeruginosa* persister cell waking. *J Appl Microbiol* **127**: 1768–1775.

Zhang, Y. (2014) Persisters, persistent infections and the Yin-Yang model. *Emerg Microbes Infect* **3**: e3.

Zhao, Y., Lv, B., Sun, F., Liu, J., Wang, Y., Gao, Y., *et al*. (2020) Rapid freezing enables aminoglycosides to eradicate bacterial persisters via enhancing mechanosensitive channel mscL-mediated antibiotic uptake. *mBio* **11**: e03239-03219.

Zheng, E.J., Stokes, J.M., and Collins, J.J. (2020) Eradicating bacterial persisters with combinations of strongly and weakly metabolism-dependent antibiotics. *Cell Chem Biol* **27**: 1544–1552.

## Supporting Information

Additional Supporting Information may be found in the online version of this article at the publisher's web-site:

**Appendix S1**: Supporting Information